Simulating Plasma-Induced Hall Thruster Wall Erosion With a Two-Dimensional Hybrid Model

Emmanuelle Sommier, Michelle K. Scharfe, Nicolas Gascon, Mark A. Cappelli, and Eduardo Fernandez

***Abstract*—A 2-D radial–axial $(r–z)$ hybrid Fluid/Particle-in-Cell (PIC) model has been developed to model energetic particle-induced channel-wall erosion in coaxial Hall discharge plasma thrusters. The discharge model geometry corresponds to that of a so-called stationary plasma thruster with an extended dielectric channel, and the computational domain extends from the anode at the base of this channel through the channel interior and into the near-field plume region. A model of the wall-erosion process has been added to the simulation in order to assess thruster degradation due to ion and energetic-neutral-induced sputtering of the channel walls. The effect of ion–neutral collisions, including momentum and charge-exchange collisions, on the erosion process is examined. These models are used to simulate the long-term wall-erosion history. For the specific Hall-thruster-configuration modeled, collisions were found to have less than a 10% effect on wall erosion. The erosion rate is seen to decrease with time, in good agreement with experimental measurements of long-term erosion in similar thrusters, resulting in a wall recession of as much as 2 mm after 4000 h of simulated operation.**

***Index Terms*—Hall thrusters, particle simulations, plasma propulsion.**

I. Introduction

HALL THRUSTERS are magnetized $\mathbf{E} \times \mathbf{B}$ plasma discharges that are currently of interest for use in space-propulsion applications. Their high specific impulse (1000–4000 s) and relatively high thrust efficiency (typically, 40%–50%) makes them ideal for long-duration missions, such as satellite station keeping and orbit transfer [1]. In these devices, the electrons drift between an external hollow cathode and an anode at the base of the annular channel. A radial magnetic field magnetizes the electrons causing an $\mathbf{E} \times \mathbf{B}$ Hall current that restrains the flow of electrons to the anode, producing a region of high ionization and strong electric field. This field accelerates the ions axially along the annular channel, generating thrust. A schematic of the Hall discharge considered in this paper, typical of most Hall thrusters, is shown in Fig. 1. This particular Hall thruster is a laboratory device, which is intended for studies of electron transport, and was instrumented with an external antenna array for performing measurements of the Hall current.

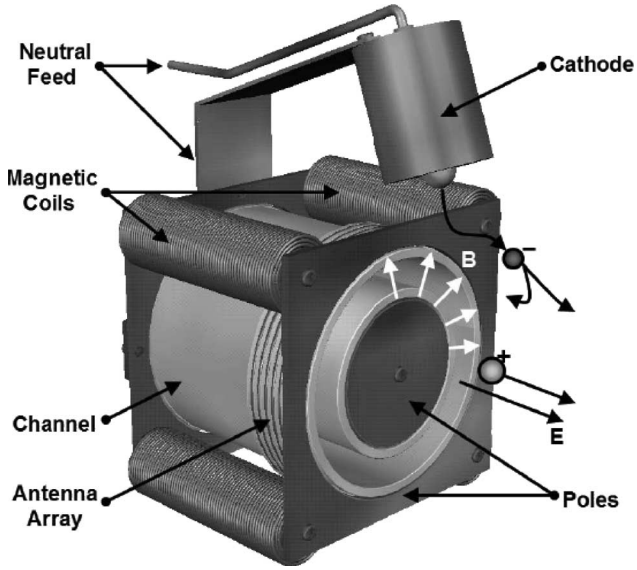

Fig. 1. Schematic of the Hall thruster plasma discharge simulated in this paper.

While these devices show great promise for future space-propulsion applications, a significant issue hindering widespread adoption is a lack of lifetime predictability. Discharge-channel wall erosion is a limiting factor in determining Hall thruster operational lifetime. A motivating factor for the development of Hall thruster simulations is to better understand and predict the time evolution of channel walls due to plasma-induced erosion. The erosion of Hall thruster channel walls is caused by the bombardment of energetic ions and neutrals, resulting in the direct sputtering of the wall material [2], [3]. Since future missions will require thruster lifetimes on the order of several years, determining this lifetime experimentally in ground-test facilities is both time-consuming and expensive, particularly when attempting to optimize operating conditions or geometry for maximum life. A robust and accurate numerical simulation is a necessary alternative for evaluating both thruster performance and life.

In this paper, a sputtering model has been introduced into a 2-D hybrid Fluid/Particle-In-Cell (PIC) simulation in order to determine the erosion behavior of the channel walls in a laboratory Hall discharge. The hybrid model used here to simulate the plasma-discharge properties is similar to that developed by other researchers [4]–[6]. The use of these hybrid models to simulate long-term erosion in Hall thrusters is relatively new, although other 1-D and 2-D fluid simulations have been

Manuscript received February 14, 2007; revised June 23, 2007. This work was supported in part by the Air Force Office of Scientific Research. The work of E. Sommier was supported by SAFRAN Company, France.

E. Sommier, M. K. Scharfe, N. Gascon, and M. A. Cappelli are with the Mechanical Engineering Department, Stanford University, Stanford, CA 94305 USA (e-mail: cap@stanford.edu).

E. Fernandez is with the Department of Mathematics and Physics, Eckerd College, St. Petersburg, FL 33711 USA.

Color versions of one or more of the figures in this paper are available online at http://ieeexplore.ieee.org.

Digital Object Identifier 10.1109/TPS.2007.905943

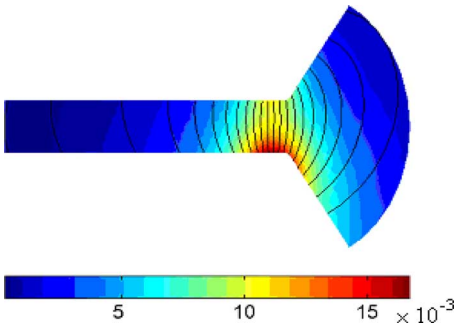

Fig. 2. Magnetic-field strength (Tesla) and magnetic contours (lines of constant field) for the Stanford Hall Thruster modeled in this paper.

used recently to also understand Hall thruster erosion [7], [8]. In the simulations presented here, we include a study of the effect of charge-exchange and momentum-exchange collisions on the sputtering process. Successive simulations that use the computed local erosion rate to update the geometry of the walls are used to predict the erosion evolution of the channel over a 4000-h period. Although experimental data for such long-term erosion is not available for the Hall thruster modeled, comparisons are made to available data for a Russian-built stationary plasma thruster (SPT-100 thruster) [9]. The present simulation, like most other hybrid simulations, assumes a static (vacuum) magnetic field imposed by the external magnetic circuit. We examine, here, the possible significance of the induced magnetic field generated by the distributed Hall current, as this field can alter the shaping of the equipotential surfaces in the discharge.

II. Numerical Model

A. Brief Overview

In order to simulate erosion of the channel walls, a sputtering model has been incorporated into an existing 2-D (radial–axial) hybrid simulation of the discharge channel and near-field plume region of a Hall-thruster plasma. The hybrid simulation, which was developed originally by Fernandez *et al.* [10], is an extension of the model of Fife [11]. A more detailed description of the model and a comparison of simulated plasma properties with experimental measurements can be found in [12]. In the model, the electrons are treated as a quasi-1-D fluid while the heavy species are treated as discrete particles advanced in space using a PIC approach. The two solutions are coupled assuming space-charge neutrality.

The computational geometry used in the simulation corresponds to a laboratory Hall discharge referred to, here, as the Stanford Hall Thruster. The annular channel is 8 cm in length and 1.2 cm in width with an outer diameter of approximately 9 cm. The peak radial magnetic field, measured with the discharge turned off, is 1.6×10^{-2} T located approximately 5-mm upstream of the channel exit along the inner wall, as shown in Fig. 2. A discharge voltage of 200 V and a xenon flow rate of 2 mg/s from the anode are simulated in order to match nominal experimental operating conditions.

The electron fluid is governed by ion and electron continuity equations, electron momentum equations parallel and perpendicular to the magnetic field, a 1-D electron energy equation, and a current continuity equation [10], [12]. The electron mobility along magnetic-field lines is assumed to be infinite, resulting in isothermal magnetic-field contours. However, the pressure-gradient contribution to electric potential in the parallel direction is included, resulting in radial, in addition to axial, electric fields. The electron-energy equation includes a Joule heating-energy-source term and accounts for energy invested in ionization and lost to electron-wall collisions.

As described by Barral *et al.* [13], determination of the electron-energy loss to the channel walls requires knowledge of the average energy per incident particle and the net electron flux including secondary electron emission. However, both the incident energy and the flux depend on the sheath potential, which is not directly simulated. Instead, the sheath potential is computed assuming an isotropic Maxwellian electron-velocity distribution in the bulk plasma and equal fluxes of ions and electrons to the dielectric channel walls. In order to reduce computational cost, the presheath is not resolved. This means that the simulated radial ion velocity at the edge of the computational boundary is well below the Bohm velocity required for a stable sheath [14]. In order to satisfy the Bohm criteria, the ions are assumed to enter the sheath at the Bohm velocity, and the simulated number density at the wall is artificially lowered to account for the ion acceleration. A more detailed description of the wall-energy losses in our model is given in [12].

A major challenge in all Hall-thruster simulations is the proper account of cross-field electron transport. It is well established that, in some regions of the channel, the electron transport is anomalous [15], but the use of a usual Bohm model for the electron mobility overpredicts the electron current near the exit of the discharge. Since the focus of this paper is in extending the model's capability in simulating wall erosion, we use an experimentally measured cross-field electron mobility (axially varying but uniform over radius), which results in model predictions of detailed plasma properties that are in reasonable agreement with experimental measurements [12]. We are presently carrying out parallel studies of the development of suitable electron-transport models that can capture the spatially varying electron mobility in the discharge channel [16].

The motion of the heavy-particle species, Xe and Xe^+, is solved in three dimensions using cylindrical coordinates. Due to the large Larmor radius of ion species, the equation of motion for the ions neglects the effect of the magnetic field and only includes a force due to the spatially varying transient electric field. Neutral particles are injected at the anode and scatter off channel walls assuming a one-way Maxwellian flux distribution at the wall temperature of 1000 K. Ions, which impact channel walls, are neutralized before being reemitted into the channel. In order to more accurately calculate the erosion, prior to impacting the channel walls, the radial component of ion velocity is enhanced through calculation of a sheath potential assuming a Bohm condition for the ion velocity at the sheath edge. Ionization and heavy-particle collisions take place everywhere inside the computational domain based on local plasma properties. In addition, neutral particles are injected from the computational boundaries in the near-field region in order to simulate a backpressure of 0.05 mTorr. Note that

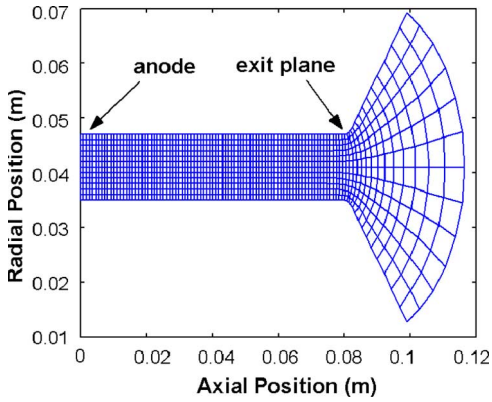

Fig. 3. Computational grid employed for 2-D hybrid simulations of the Stanford Hall Thruster.

adding background neutrals affects the results mostly outside of the channel (for a detailed analysis of the influence of backpressure on the simulation, the interested reader is referred to the paper by Scharfe *et al.* [12]).

The computational domain used to simulate a slice of the radial axial plane extends from the anode located at the base of the channel, through the interior of the channel, and into the near-field plume region. The computational grid consists of 100 cells in the axial direction and 12 cells in the radial direction, as shown in Fig. 3. As aforementioned, the coarseness of this grid near the channel walls does not capture the potential drop due to the presheath. Simulations using a refined grid near the wall, at the expense of increased computational time, have shown that accurately modeling this region has only a small effect on bulk properties, such as electron temperature and potential. The radial acceleration due to the presheath may cause the radial velocity of incident ions near the exit plane to increase by as much as 3000 m/s. While this increase will likely only have a small effect on the incident energy of the impacting ions, which have an axial velocity of nearly 10 000 m/s at the exit plane, an underestimate of this radial-velocity component by not satisfying the Bohm condition can impact the determined incidence angle and, therefore, the sputter yield. Future work will examine the influence of the presheath and sheath on erosion more closely.

For computational manageability, macroparticles are used to represent large groups of neutrals and ions rather than simulating individual particles. Since neutral and ion densities differ by orders of magnitude over the length of the domain, the statistical weighting of the macroparticles (i.e., how many actual particles are represented by a macroparticle) vary with position and with the species represented (i.e., neutrals or ions). The simulation is initialized with approximately 500 000 neutral macroparticles and 350 000 ion macroparticles. The ion and neutral time step is typically 25 ns, while the electron time step is 0.1 ns.

The total amount of simulated time is 625 μs, which takes one day to compute on a single processor (AMD Athlon 64–3500 MHz) desktop computer. This time could be reduced by optimizing the code, which will be the subject of future work. Representative results of ion-density distribution (color map) and ion velocity (superimposed vectors) averaged over time are illustrated in Fig. 4. An examination of Fig. 4 indicates that the plasma density is highest approximately 2–3 cm upstream of the channel exit. However, erosion takes place mainly in the last centimeter of the channel, since only the ions in this region have accelerated to a sufficiently high energy to induce sputtering.

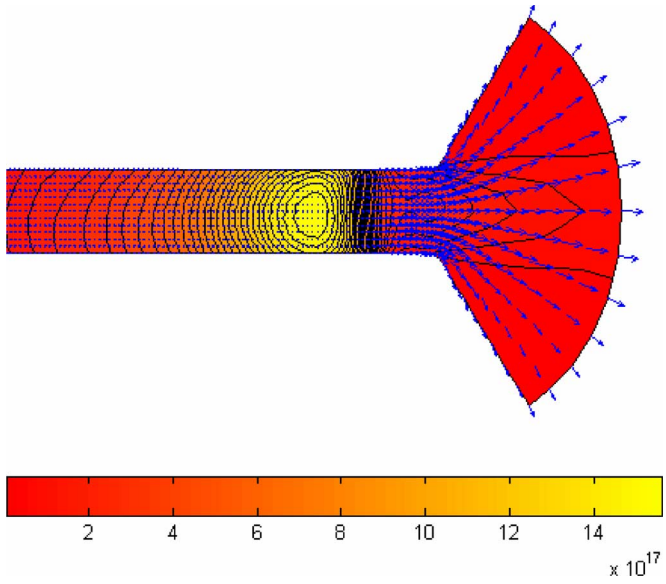

Fig. 4. Computed ion density (m^{-3}) and superimposed ion velocities.

B. Erosion Model

The erosion of the thruster walls is modeled by considering the sputter processes associated with energetic particle bombardment of the channel. Sputtering requires enough incident particle kinetic energy to overcome the interatomic binding energy of the atoms at the solid surface. The number of atoms ejected from the surface per incident particle is the sputter yield, often measured in removed volume per incident charge (in cubic meters per Coulomb), as most experiments are carried out for energetic ions. In addition to the incident particle-mass and target-surface composition, the sputter yield depends most strongly on the incidence angle and energy of the particle. Experimental data for sputter yields of ions/atoms on materials of interest to Hall thruster applications is rare, most notably at the incident energies of interest ($\leq$ 300 eV), and the reader is referred to the study of Yim *et al.* [8], which discusses, in more detail, the available data and the sensitivity of erosion calculations to the sputter-yield thresholds.

For every increment of time, the number of particles sputtered from the wall at an axial position z is modeled as

$$S(z) = \frac{\sum_{\phi,\varepsilon} S_\phi(\phi) \cdot f(\phi,\varepsilon,z) \cdot S_\varepsilon(\varepsilon)}{\sum_{\phi,\varepsilon} f(\phi,\varepsilon,z)}. \quad (1)$$

Here, $S_\phi(\phi)$ and $S_\varepsilon(\varepsilon)$ are angular and energy-dependent sputter yields, respectively, as shown in Fig. 5 for singly ionized Xe incident onto boron nitride (BN). Since we allow for the possibility of sputtering due to energetic neutrals formed by charge exchange, we represent $S_\phi(\phi)$ in the usual way, as normalized

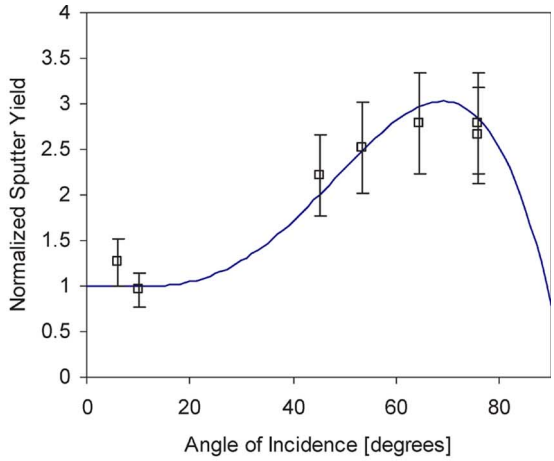

(a)

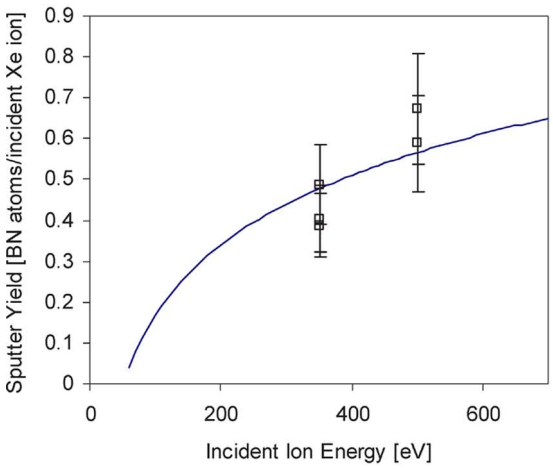

(b)

Fig. 5. (a) Normalized sputter-yield angular dependence and (b) energy dependence for xenon on BN. Solid lines represent curve fits [7] to the data of Garnier *et al.* [17].

at zero incident angle and $S_\varepsilon(\varepsilon)$ as a sputter probability (i.e., atom sputtered per incident ion or neutral) by taking an atom density of 1.05×10^{29} atoms/cm^3 for hexagonal BN. The solid curves in Fig. 5 are fits in accordance with those recommended by Manzella *et al.* [7], which were used in 1-D fluid simulations of erosion in SPT-100. In addition, shown in Fig. 5 is the experimental data of Garnier *et al.* [17] for xenon ions on BN. In (1), $f(\phi, \varepsilon, z)$ represents the local angle and energy distribution of the particles (neutrals or ions) incident onto the surface over the same time increment, which is normalized at each position by the total number of particles (neutrals or ions) impacting the wall at this position. Ions with energy greater than the characteristic threshold energy of 50 eV (e.g., xenon ions on BN) participate in the sputtering process. We assume that energetic neutral particles can also cause sputtering, and we use the same energy-dependent yield as that for ions, shifted to higher energy by the ionization energy of the atom. The ionization energy is added to the sputter-yield threshold to account for the absence of energy released through electron capture.

At a position z along the channel, the erosion rate is obtained from the product of $S(z)$ and the incident flux $\Gamma(z)$ of energetic particles

$$R_{\text{wall}} = S(z) \cdot \Gamma(z). \tag{2}$$

The incident wall flux is related to the particle-distribution function by

$$\Gamma(z) = \sum_{\phi,\varepsilon} \frac{f(\phi, \varepsilon, z)}{\delta A(z) \delta t}. \tag{3}$$

Here, $\delta A(z)$ is the discretized annular wall area at a position z, and δt is the time in the simulation over which the distribution function is evaluated.

The sputtering model has been integrated into the thruster simulation as follows. Particle (ion and neutral) positions and velocities are updated at each time step. If a particle is found outside the boundaries of the computational domain, the position where the particle crossed the boundary is found in order to determine if a wall collision occurred. In these situations, the energy and incidence angle of the impacting particle are then calculated. If, in addition, the particle is energetic enough to contribute to the sputtering process, it is included in the local-distribution function, which is used to determine the sputter rate. The instantaneous spatially varying erosion rate is then calculated from the rate at which these particles collide with the surface in accordance with (2) above.

It is found from the simulations that nearly all of the erosion, due mainly to high-energy ions, occurs in a region very near the thruster exit. This is confirmed by examining the average ion energy along the walls of the channel (Fig. 6). The peak in ion energy for both the inner and outer insulator walls is observed in a region near the channel exit. Therefore, in order to further increase the spatial resolution of the erosion process beyond the cell dimensions used in the PIC model, the 1-cm-long region where most sputtering occurs has been divided into 14 segments. At each segment position, the model calculates the distribution function of the high-energy particles impacting the walls and deduces the wall flux, sputter yield, and the local wall-erosion rate. The walls are subsequently advanced (with a corresponding computational-grid adjustment), and the plasma and thruster properties are then recomputed for the modified geometry.

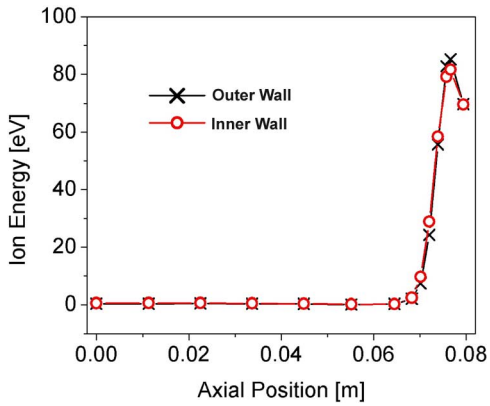

Fig. 6. Average ion energy on the thruster channel walls.

C. Ion–Neutral Collisions

To improve accuracy, both charge- and momentum-exchange collisions are included in the simulation. The former is found to have a significant effect on the results of the simulation, since charge-exchange collisions alter the energy distribution of ions and neutrals. During a charge-transfer event, a slow neutral and a fast ion will become a fast neutral and a slow ion, respectively. Elastic momentum-exchange collisions alter the energy-distribution functions of each species to a far lesser extent. However, since a change in incidence angle of an impacting particle modifies the sputter yield, momentum exchange collisions were included to understand their role in altering the sputtering process. Since neutrals are much slower than ions in the last centimeter of the channel, the importance of elastic momentum-exchange collisions increases in the region where erosion is prevalent.

In order to implement heavy-particle collisions in the hybrid simulation, the collision probability in each cell is determined by the no-time-counter method of Bird [18]. Measurements by Miller *et al.* [19] are used to determine the total charge-exchange cross section as a function of energy

$$\sigma_{\text{cex}} = \left(-13.6 \log_{10}\left(\frac{m_{\text{Xe}} g^2}{2e}\right) + 87.3\right) \times 10^{-20}\ \text{m}^2. \quad (4)$$

Here, σ is the total charge-exchange cross section, and g is the relative speed. The cross section used for elastic collisions is that of Boyd and Dressler [20]

$$\sigma_{\text{el}} = \frac{6.42 \times 10^{-16}}{g}\ \text{m}^2. \quad (5)$$

1) Charge-Exchange Collisions: On average, a neutral macroparticle is two orders of magnitude larger than an ion macroparticle. Therefore, if a charge-exchange collision is determined to take place, the larger particle (typically the neutral) is divided into a small particle that has the statistical weight of the collision partner and a larger particle containing the balance of the atoms/ions. Since the most probable scattering event involves very little momentum transfer, the precollision velocities of the ion and neutral macroparticles of the same statistical weight are exchanged, while the remainder of the larger macroparticle keeps the same precollision velocity as it is not assumed to be subjected to a collision. Although this process removes fast ions, which may contribute significantly to the sputtering process, it produces high-energy neutrals, which may also play a role in the erosion process and cannot necessarily be neglected.

Fig. 7 shows that, with charge-exchange collisions, the incident-wall ion-energy distribution is shifted toward lower energies near the exit, as expected. Concomitant with this decrease in ion velocity is a decrease in ion density, as shown in Fig. 8. This decrease in ion density is attributed to a decrease in average neutral density, since the neutral velocity increases due to charge exchange. The overall affect of charge-exchange collisions is, therefore, to cause a decrease in the thrust, the primary component of which is due to the ion-momentum flux.

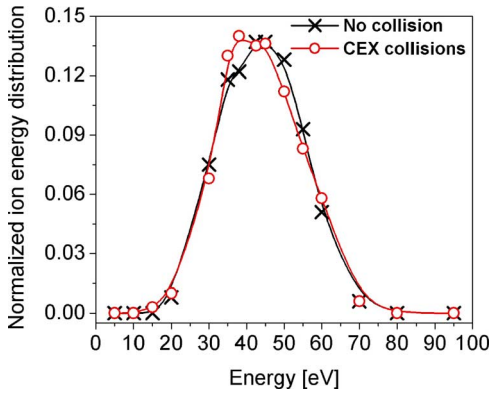

Fig. 7. Computed ion-energy distribution (with and without charge-exchange collisions) at the outer wall at a position of 7 mm upstream of the exit plane.

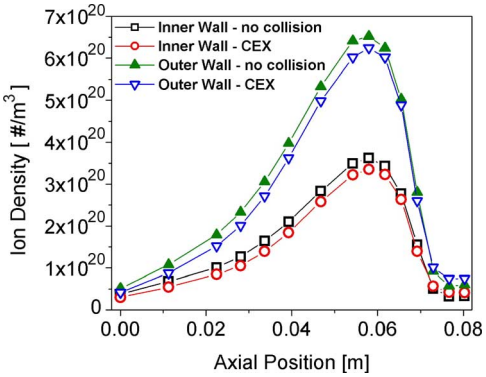

Fig. 8. Computed ion density at the inner and outer wall (with and without charge-exchange collisions).

TABLE I
COMPARISON BETWEEN THE AVERAGE VALUES OF COMPUTED PERFORMANCE DATA FOR SIMULATIONS WITH AND WITHOUT COLLISIONS

	No collision	CEX collisions	CEX and MEX collisions
Discharge Current [A]	2.3	2.0	2.1
I_{sp} [s]	1400	1210	1240
Thrust [mN]	27.5	23.7	24.4

2) Momentum-Exchange Collisions: Similar to the treatment of charge-exchange collisions, for momentum-exchange collisions, the larger macroparticle is divided into two smaller macroparticles, where one particle is the same statistical weight as its collision partner. In the treatment of the momentum-exchange process, the particles preserve relative speed and collide in accordance with a variable hard-sphere model to determine postcollision velocities.

3) Effects of Collisions on Thruster Performance: In the simulation, the thrust is calculated as the force produced on ions by the electric field in the entire simulation domain. As a consequence, the thrust neglects the momentum of injected neutrals and includes a negative thrust due to the ambipolar diffusion-driven backflow of ions close to the anode.

The first effect of collisions on the thruster performance is a reduced thrust and specific impulse compared to a model with no collisions, as shown in Table I. As discussed earlier, this is mainly due to charge-exchange collisions decreasing the

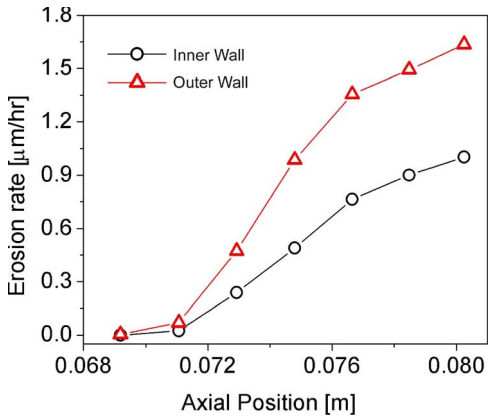

Fig. 9. Computed initial inner and outer wall erosion rate.

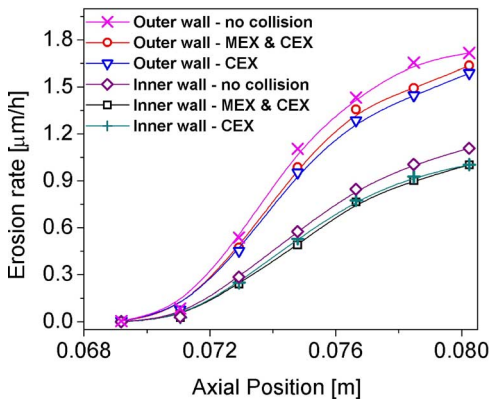

Fig. 10. Effect of particle collisions on the erosion rate of the outer wall.

number of fast ions producing thrust, through a decrease in the ion density. Momentum-exchange collisions may also affect the thrust, since momentum-exchange collisions can modify the direction of ion velocity, the axial component of which contributes to the thrust. However, as shown in the table, the contribution of momentum-exchange collisions to the overall impact that collisions have on thrust is seemingly small.

III. Results and Discussion

Using the described sputtering model, simulated erosion rates due to neutrals and ions have been obtained including the effects of collisions. The sputtering due to energetic neutrals appears to be about 1000 times smaller than the rate of sputtering due to ions. As a result, the following discussion about wall sputtering and erosion focuses mainly on the role played by energetic ions.

The computed wall-erosion rate is given in Fig. 9. It is apparent from Fig. 9 that sputtering is more prevalent on the outer wall than on the inner wall, suggesting that, if the wall thickness is comparable, through-wall erosion would take place first on the outer wall. The origin for this asymmetry is attributed to the shape of the magnetic-field distribution within the channel and the subsequent ion trajectories as they accelerate through the potential distribution from the position at which they are created. The magnetic-field distribution used in this particular thruster shows a greater lensing of the magnetic field (and, hence, equipotential lines), directing ions away from the inner wall a distance of 1–2 cm upstream of the exit plane (see Fig. 2). It is noteworthy, however, that the potential contours are not only affected by the magnetic-field distribution but also by the plasma-density distribution and by gradients in the electron temperature.

The results presented in Fig. 10 serve as a means of examining the effects of collisions (both charge exchange and momentum exchange) on the overall erosion process. A general consequence of charge-exchange collisions is a lowering of the maximum erosion rate by approximately 10%, which is caused by a reduction in the population of high-energy ions scattering with the walls. Momentum-exchange collisions slightly increase the erosion rate. This increase is due to the collisional redirection of ions (accelerated primarily along the axial direction) toward the walls.

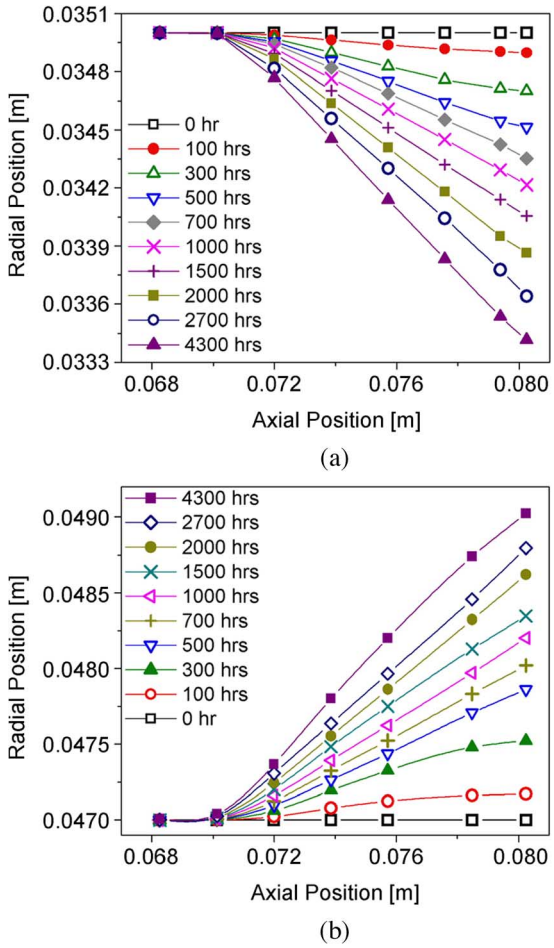

Fig. 11. Simulation of the channel-wall recession due to erosion. (a) Inner wall. (b) Outer wall.

Fig. 11 presents a computational simulation of the erosion history of the inner and outer thruster walls. The simulations were carried out to an effective thruster operating time of 4300 h. It is observed that the erosion rate decreases substantially over time, with more than half of the erosion occurring in the first 1000 h of life. This result is in qualitative agreement with calculations using a 2-D fluid model of an SPT-100 thruster [8]. The drop in the instantaneous erosion rate is believed to be primarily caused by the angular dependence of

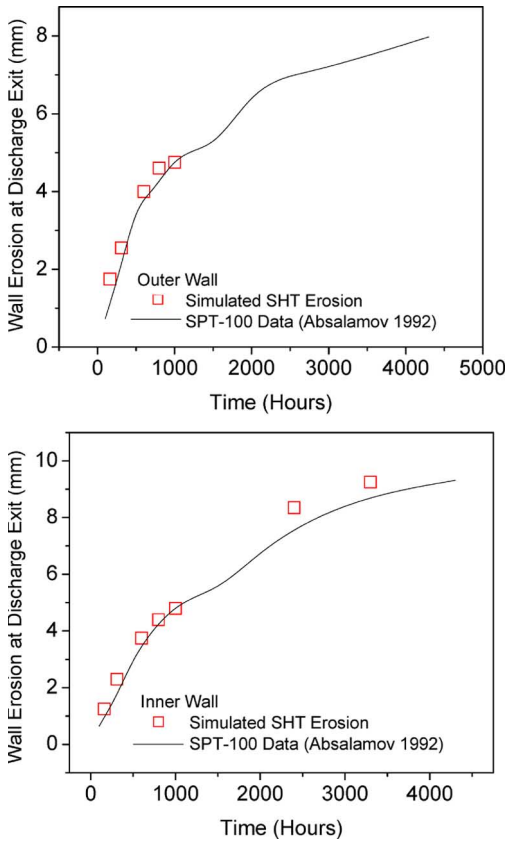

Fig. 12. Comparison of the predicted (solid line) erosion variation with time at the exit of the SHT to that measured for an SPT-100 thruster (symbols, Absalamov 1992 [10]). Note that the predicted erosion is scaled to that for the SPT-100 at 1000 h for this comparison.

the sputter yield, which is maximized for an incidence angle of about 65° relative to the surface normal (Fig. 5). Since the erosion rate decreases as the relative incidence angle increases due to sputtering, this implies that the majority of high-energy ions contributing to sputtering have incident angles greater than 60° relative to the surface normal. It is noteworthy that, by 4300 h, the surface is predicted to erode to an angle of about 11° relative to the thruster axis.

The lack of available long-term erosion data for the thruster modeled here precludes a direct comparison of the predicted erosion history to experimental data. Furthermore, it has been documented that differences in erosion rates are seen with channel walls made with varying grades of BN [21]. It is not yet clear if these differences are due to differences in sputter yield or to differences in the electron-emission properties which affect the discharge operation. This interplay and sensitivity to specific material grade makes a direct simulation of the absolute rate of erosion difficult. However, it is interesting to compare our results with data collected from a life-test carried out on an SPT-100 thruster [9] (which is typically operated with a borosil channel—a composite of BN and silica, with other minor constituents), data that was later verified by an SPT-100 endurance test in the U.S. [22]. While the overall erosion rate is expected to be higher for the SPT-100, a commercial thruster operating at much higher efficiency and ion current than the thruster used here, we would expect that the variation in the erosion rate with time should be similar. Fig. 12 compares

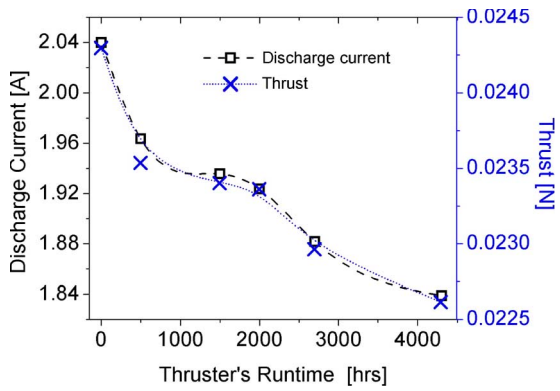

Fig. 13. Predicted discharge current and thrust variation over the life of the thruster.

the measured time-dependent erosion at the exit of the channel for the SPT-100 to that computed here, with the predicted erosion for our thruster scaled to that of the SPT-100 at a time of 1000 h. It is noteworthy that the agreement is remarkable, despite the difference between these thrusters (size, power, etc.) and that no adjustments have been made in the angular and energy-dependence of the sputter yields used to model the erosion process. At this time, we cannot determine whether this agreement is merely coincidental or if it reveals a general feature of Hall thruster erosion.

In addition to influencing thruster lifetime, the erosion process is expected to affect the discharge operation and thruster performance. Therefore, the effects of channel-wall erosion have been studied by examining the evolution of the simulated discharge current and the thrust for an operating time of 4300 h. As shown in Fig. 13, the performance of the thruster decreases as the wall is eroded, primarily as a result of diminished discharge current, which is attributed to a gradual decrease in the plasma density. A similar drop in thrust with time is seen in the 2-D fluid simulations of Yim *et al.* [8].

In the simulation results discussed above, the effect of the azimuthal current on the magnetic field is ignored as it is, in most if not all, 1-D and 2-D $(r–z)$ simulations of Hall thrusters. Since the peak azimuthal Hall current is estimated to be 10–100 A for the geometry considered, the influence of the induced magnetic field on the trajectories of the ions should be examined.

In order to incorporate the induced magnetic field, the azimuthal current is first calculated using simulated plasma properties, i.e., the plasma electron density (n_{e}), the axial electric field E_z, and the radial magnetic field B_{r}

$$J_{\mathrm{az}} = e n_{\mathrm{e}} \frac{E_z}{B_{\mathrm{r}}}. \tag{6}$$

Here, e is the electron charge. The computed azimuthal current density is shown in Fig. 14. It is noted that this computed current density is about a factor of three lower than recent experimental measurements of current density using a non-intrusive antenna and fast-current-interruption technique [23]. The computed azimuthal current density has been incorporated into the simulation using the Finite-Element Method Magnetics software package [24] to evaluate the potential contribution

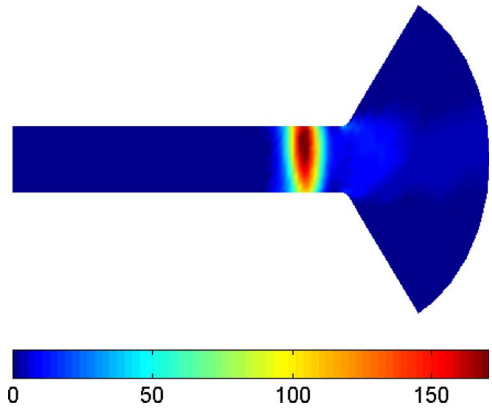

Fig. 14. Color map of the computed azimuthal Hall current density, $J_{\rm az}(\mathrm{A}\cdot\mathrm{cm}^{-2})$.

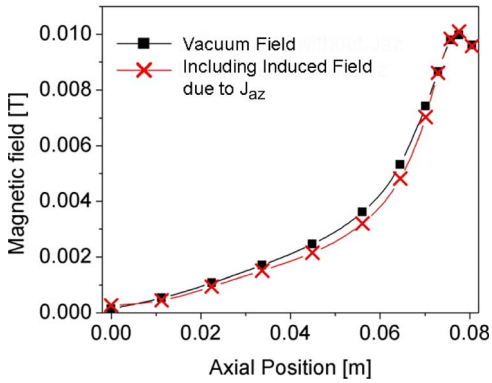

Fig. 15. Comparison of the static-vacuum magnetic field (black squares) to that computed including the azimuthal Hall current $(J_{\rm az})$, as shown in Fig. 14.

of the induced magnetic field to the total field within the channel. A comparison is made in Fig. 15 of the original externally imposed (vacuum) magnetic field and that including the calculated induced field. It is apparent that this correction is small, and simulations carried out with the corrected magnetic field have shown that this adjustment has only a minor effect on the computed wall erosion. However, as the accuracy of the simulation improves, providing better agreement with the higher Hall currents experimentally measured, the perturbation to the magnetic field may increase and the effect of the Hall current on wall erosion will need to be reexamined.

IV. Summary

We have presented a numerical simulation of the progression of erosion in a Hall thruster channel in an attempt to better understand thruster reliability and operational lifetime. This simulation incorporates a model of ion and energetic-neutral-induced sputtering into a 2-D hybrid Fluid–PIC description that accounts for energy and angular dependence in the sputter yields. The ion–neutral charge-exchange and momentum-exchange collisions are accounted for explicitly, as the former is found to have a significant effect on the instantaneous wall-erosion rate. Although energetic neutrals can be formed through these charge-exchange processes, they seem to have a negligible direct impact on the overall sputtering/erosion process. However, these energetic neutrals do result in a lower neutral density and, subsequently, lower ion density in addition to the lowered average ion velocity, which culminates as a reduction in the erosion rate as well as a reduction in the thruster performance. In contrast, momentum-exchange collisions appear to have less significance in both the wall-erosion process and on thruster performance.

At conditions studied for our laboratory thruster, differences in the erosion rate of the inner and outer walls were found to be attributed to differences in wall plasma density and not ion energy. The inner and outer wall plasma density is largely controlled by the shape of the magnetic field. While the simulated erosion rate of the inner and outer wall over thousands of hours of operation cannot be compared directly to experiments for this laboratory thruster, comparisons are made to available data for an SPT-100 thruster of the variation in the relative erosion rate over the estimated life of the thruster. Very good agreement is obtained between the erosion trends, despite differences in operating conditions and thruster geometry. This suggests that there may be a fundamental parameter that is common to most thrusters that establishes this trend.

Finally, a preliminary study of the possible effect on erosion of the induced magnetic field due to the azimuthal (Hall) current seems to suggest that this effect may be small. However, since the simulation underpredicts the Hall current in comparison to recent measurements, general conclusions regarding the role of induced magnetic fields on performance and erosion cannot be made at this time.

References

[1] F. S. Gulczinski, III and R. A. Spores, "Analysis of Hall-effect thrusters and ion engines for orbit transfer missions," presented at the 32nd AIAA Joint Propulsion Conf., Lake Buena Vista, FL, Jul. 1–3, 1996, AIAA-1996-2973.

[2] V. Baranov, Y. Nazarenko, and V. Petrosov, "The wear of the channel walls in Hall thrusters," presented at the Int. Electric Propulsion Conf., Pasadena, CA, Oct. 14–19, 2001, IEPC-2001-048.

[3] A. I. Morozov and V. V. Savelyev, "Fundamentals of stationary plasma thruster theory," *Rev. Plasma Phys.*, vol. 21, p. 203, 2000.

[4] F. I. Parra, E. Ahedo, J. M. Fife, and M. Martinez-Sanchez, "A two-dimensional hybrid model of the Hall thruster discharge," *J. Appl. Phys.*, vol. 100, no. 2, pp. 023 304-1–023 304-11, Jul. 2006.

[5] J. Bareilles, G. J. M. Hagelaar, L. Garrigues, C. Boniface, J. P. Boeuf, and N. Gascon, "Critical assessment of a two-dimensional hybrid Hall thruster model: Comparisons with experiments," *Phys. Plasmas*, vol. 11, no. 6, pp. 3035–3046, Jun. 2004.

[6] J. W. Koo and I. D. Boyd, "Computational modeling of stationary plasma thrusters," presented at the 39th AIAA Joint Propulsion Conf., Huntsville, AL, Jul. 20–23, 2003, AIAA-2003-10113.

[7] D. Manzella, J. Yim, and I. Boyd, "Predicting Hall thruster operational lifetime," presented at the 40th AIAA Joint Propulsion Conf., Fort Lauderdale, FL, Jul. 11–14, 2004, AIAA 2004-3953.

[8] J. T. Yim, M. Keidar, and I. D. Boyd, "An investigation of factors involved in Hall thruster wall erosion modeling," presented at the 42nd AIAA Joint Propulsion Conf., Sacramento, CA, Jul. 9–12, 2006, AIAA-2006-4657.

[9] S. K. Absalamov, V. B. Andreev, T. Colbert, M. Day, V. V. Egorov, R. U. Gnizdor, H. Kaufman, V. Kim, A. I. Koriakin, and K. N. Kozubskii, "Measurement of plasma parameters in the stationary plasma thruster (SPT-100) plume and its effect on spacecraft components," presented at the 28th AIAA Joint Propulsion Conf., Nashville, TN, Jul. 6–8, 1992, AIAA 92-3156.

[10] E. Fernandez, M. A. Cappelli, and K. Mahesh, "2-D simulations of Hall thrusters," in *CTR Annual Research Briefs*. Palo Alto, CA: Stanford Univ., 1998, p. 81.

[11] J. M. Fife, "Nonlinear hybrid-PIC modeling and electrostatic probe survey of Hall thrusters," Ph.D. dissertation, Aeronautics Astronautics Dept., MIT, Cambridge, MA, 1998.
[12] M. K. Scharfe, N. Gascon, M. A Cappelli, and E. Fernandez, "Comparison of hybrid Hall thruster model to experimental measurements," *Phys. Plasmas*, vol. 13, no. 8, pp. 083 505-1–083 505-12, Aug. 2006.
[13] S. Barral, K. Makowski, Z. Peradzynski, N. Gascon, and M. Dudeck, "Wall material effects in stationary plasma thrusters. II. Near-wall and in-wall conductivity," *Phys. Plasmas*, vol. 10, no. 10, pp. 4137–4152, Oct. 2003.
[14] D. Bohm, *The Characteristics of Electrical Discharges in Magnetic Fields*. New York: McGraw-Hill, 1949, p. 13.
[15] N. Meezan, W. Hargus, and M. Cappelli, "Anomalous electron mobility in a coaxial Hall discharge plasma," *Phys. Rev. E, Stat. Phys. Plasmas Fluids Relat. Interdiscip. Top.*, vol. 63, no. 2, p. 026 420, Feb. 2001.
[16] M. K. Allis, C. Thomas, N. Gascon, M. Cappelli, and E. Fernandez, "Introduction of physical transport mechanisms into 2D hybrid Hall thruster simulations," presented at the 42nd AIAA Joint Propulsion Conf., Sacramento, CA, Jul. 9–12, 2006, AIAA-2006-4325.
[17] Y. Garnier, V. Viel, J.-F. Roussel, and J. Bernard, "Low-energy xenon ion sputtering of ceramics investigated for stationary plasma thrusters," *J. Vac. Sci. Technol. A, Vac. Surf. Films*, vol. 17, no. 6, pp. 3246–3254, Nov. 1999.
[18] G. A. Bird, *Molecular Gas Dynamics and the Direct Simulation of Gas Flow*. Oxford, U.K.: Oxford Science, 1994.
[19] J. S. Miller, S. H. Pullins, D. J. Levandier, Y. Chiu, and R. A. Dressler, "Xenon charge exchange cross sections for electrostatic thruster models," *J. Appl. Phys.*, vol. 91, no. 3, pp. 984–991, Feb. 2002.
[20] I. D. Boyd and R. A. Dressler, "Far field modeling of the plasma plume of a Hall thruster," *J. Appl. Phys.*, vol. 92, no. 4, pp. 1764–1774, Aug. 2002.
[21] P. Y. Peterson and D. H. Manzella, "Investigation of the erosion characteristics of a laboratory Hall thruster," presented at the 39th Joint Propulsion Conf., Huntsville, AL, Jul. 20–23, 2003, AIAA-2003-5005.
[22] C. E. Garner, J. R. Brophy, J. E. Polk, and L. C. Pless, "Performance evaluation and life testing of the SPT-100," presented at the 30th Joint Propulsion Conf., Indianapolis, IN, Jun. 27–29, 1994, AIAA-94-2856.
[23] C. A. Thomas, N. Gascon, and M. A. Cappelli, "The non-intrusive characterization of the azimuthal drift current in a coaxial E × B discharge plasma," *Phys. Rev. E, Stat. Phys. Plasmas Fluids Relat. Interdiscip. Top.*, vol. 74, no. 5, p. 056 , Nov. 2006.
[24] FEMM, *Finite Element Method Magnetics*, 2004, Boston, MA: Foster-Miller, Inc. Software Package, Version 4.0.

Emmanuelle Sommier received the degree in engineering from Ecole Nationale Superieure de Mecanique et D'Aerotechnique, Poitiers, France, in 2003.

She was a Visiting Researcher with Stanford University, Stanford, CA, from 2004 to 2006. Her research focused on the development of robust simulations for modeling erosion behavior in Hall plasma thrusters.

Michelle K. Scharfe received the B.S. degree in engineering and applied science from the California Institute of Technology, Pasadena, in 2003 and the M.S. degree in mechanical engineering from Stanford University, Stanford, CA, in 2005, where she is currently working toward the Ph.D. degree.

Her research interests are in improving Hall-thruster simulations through inclusion of more accurate physics, particularly in the areas of electron transport, heavy-particle dynamics, and electron–wall interactions.

Nicolas Gascon received the Ph.D. degree in radiation and plasma physics from the University of Provence, Marseilles, France.

He joined the Stanford Plasma Physics Laboratory in 2001. He is currently a Research Associate in the Mechanical Engineering Department, Stanford University, Stanford, CA. His research projects focus on understanding the physics of magnetized discharges, anomalous electron transport, plasma–wall interactions, and developing novel plasma-propulsion concepts.

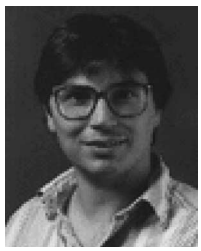

Mark A. Cappelli received the B.A.Sc. degree in physics from McGill University, Montreal, QC, Canada, and the M.A.Sc. and Ph.D. degrees in aerospace science from the University of Toronto, Toronto, ON, Canada.

He is currently a Professor of mechanical engineering with Stanford University, Stanford, CA, where he has been since 1987. His research interests include plasma physics and spectroscopy, plasma propulsion, plasma-assisted combustion, and plasma-assisted material synthesis.

Eduardo Fernandez received the B.S. degree in physics and mathematics from the University of Wisconsin–Eau Claire, Eau Claire, and the Ph.D. degree in physics from the University of Wisconsin–Madison, Madison.

He did postdoctoral work on plasma simulation with the Center for Turbulence Research, Stanford University, Stanford, CA, where he develop a two-dimensional hybrid Hall-thruster code. He is currently an Associate Professor of physics and mathematics with the Department of Mathematics and Physics, Eckerd College, St. Petersburg, FL, where he has been since 1999. Besides electric propulsion, his research interests include turbulence in fluids and plasmas.